



Thermal, mechanical and electrical performance of structural epoxy resins filled with carbon nanofibers

Liberata Guadagno¹ · Carlo Naddeo¹ · Marialuigia Raimondo¹

Received: 12 March 2023 / Accepted: 19 August 2023 / Published online: 16 September 2023
© The Author(s) 2023

Abstract

Carbon nanofibers (CNFs) were heat-treated at 1100 °C (CNF1100) and 2500 °C (CNF2500), respectively, and embedded as fillers at different mass percentages into an epoxy mixture. The paper aims at evaluating, through a comparison between the two different types of resulting nanocomposites, the influence of the CNF heat treatment on the thermal, mechanical, and electrical performance of the formulated samples. Thermogravimetric analysis (TGA) showed oxidative stability in the air of CNF2500 approximately 200 °C higher than the CNF1100 ones. The first oxidation stage of the resins embedding the two typologies of CNFs falls between 380 and 480 °C. This means that the temperature of the heat treatment of the nanofiller does not influence the temperature at which the thermodegradation of the nanocomposites starts. Differential Scanning Calorimetry (DSC) data show that the highest degree of cure (DC) was recorded for the epoxy samples filled with CNF2500. CNF thermal treatment increases the direct current (dc) conductivity of the nanocomposite by 3 orders of magnitude around the electrical percolation threshold (EPT) and increases the storage modulus of the CNF2500-based resins up to 60 °C compared with the unfilled resin. The peculiar wall structure of CNF1100 determines a further slight enhancement. Tunneling Atomic Force Microscopy (TUNA) reveals that the CNFs are evenly distributed on the nanodomains showing higher electric current values for samples loaded with CNF2500.

Keywords CNF-based epoxy resins · Thermal analysis · Mechanical and electrical properties · Thermosetting resins · Tunneling atomic force microscopy (TUNA)

Introduction

Researchers and industrialists are increasingly focusing their interest on epoxy resin-based composites because they are versatile materials with competitive materials in terms of thermal, chemical and physical properties [1–10]. The exceptional mechanical properties and considerable structural stability make them ideal candidates for various applications such as automotive, aeronautics, marine industry, electronics and others [11–18]. In this context, the concept of multifunctional composites has become a priority in recent years and is accompanied by several definitions. The most common is that of a material, a structure, or a set of materials capable of performing different functions through an intelligent combination of a structural function

with one or more additional functional capabilities, depending on system requirements. The most practical approaches start from conventional structures, to which they add layers, microsystems, and/or devices that enhance functionality [19, 20]. It is worth noting that epoxy resin-based materials can be suitably addressed to achieve desirable properties that can face future challenges through a targeted choice of synthetic precursors and fillers, as well as polymerization cycles and incorporation methods. In this context, in the last years, the issue of recycling thermosets has also been addressed, especially from the perspective of recovering valuable fillers [21–23]. Although this issue is still an unsolved problem, some technologies developed at a lab scale are considered suitable for large-scale recycling of the most commonly used thermoset composites, allowing the most precious reinforcing fibers to be recovered. It is worth noting that the difficulty in recycling is due to the crosslinked three-dimensional chemical nature of the thermoset matrix that cannot be remelted using heat or solvent, as it happens for thermoplastic matrices. Hence recycling is often an expensive and low-rate

✉ Marialuigia Raimondo
mraimondo@unisa.it

¹ Department of Industrial Engineering, University of Salerno,
Via Giovanni Paolo II, 132, 84084 Fisciano, Italy

process. However, different research activities have been proposed for the hydrolytic polymerization of epoxy resins in raw monomers. Thermoset recycling has become necessary and must continue to be investigated to become an environmentally friendly and financially convenient solution for waste management [24].

In the case of nanostructured polymers and nanocomposites, it is of fundamental importance to search for an effective matrix-nanoparticle interaction to ensure excellent performance in the final material. In this regard, the complete dispersion of the nanoparticles in the matrix and the consequent realization of a large interface area are crucial. Among the nanofillers, particular attention has been addressed to several nanostructured forms of carbon. Carbon nanomaterials, from high to low technology, are used in various engineering applications [25–27]. Films are used as tribological coatings [28]; fibers are used in composites for their strength [29]; and nanotubes and graphene are being explored for use in microelectronics [30]. It is also worth mentioning the possibility of chemically functionalizing the fibers or nanoparticles using sol–gel techniques [31]. The sol–gel method is a conventional and industrial method for synthesizing nanoparticles with different chemical compositions [32, 33]. Due to its unique properties and characteristics, this method can give high-quality nanoparticles of the same size on an industrial scale [34].

Within the class of carbon nanostructured materials, carbon nanotubes (CNTs) have aroused great interest from researchers as they have relevant physical and mechanical properties. They have encouraged many researchers to develop advanced composite materials to transfer some of the excellent physical properties of CNTs [35–38] to polymeric matrices, thus offering the possibility of combining interesting complementary properties. As conductive nanoparticles with a high aspect ratio, the efficacy of CNTs is superior to that of traditional carbon black [39, 40]. This implies that, using carbon nanotubes, composite materials characterized by high electrical conductivity at lower filler concentrations [35] can be obtained. In addition to CNTs, carbon nanofibers CNFs are also gaining attention as nanofillers for epoxies. Compared to carbon nanotubes, although they do not have a perfect structure and are less conductive, they are however quite economical in the production of epoxy resins as they offer many advantages, i.e., they are easier to disperse, process and functionalize while simultaneously guaranteeing improvements in mechanical and electrical properties [41, 42] and a lower overall cost of use. Carbon nanofibers, by virtue of their chemical structure, their compatibility with many polymeric matrices and their versatility, are increasingly being used for aircraft structures. In order to achieve a tolerance similar to that of the metal alloy, carbon nanofibers need to be properly designed to ensure efficient lightning protection. The electrical properties of

CNF-based epoxy nanocomposites are influenced by the defect sites present along the walls of the nanofibers. The investigation of the dc conductivity beyond the EPT puts in evidence a remarkable difference (about 3 orders of magnitude) between the two analyzed CNF types. This result leads to consider that the thermal treatment applied to CNFs induces a significant enhancement of the conductive properties of the CNF2500/composites for which instead it causes a lower reinforcing effect in the storage modulus than for the samples filled with CNF1100. In this study, both untreated carbon nanofibers (CNF1100)/epoxy resins and heat-treated carbon nanofibers (CNF2500)/epoxy resins were prepared by loading the fillers CNF1100 and CNF2500 with mass fractions ranging from 0.05% to 2.0%, which have been effectively dispersed in the same matrix formulation by sonication. The thermal, mechanical and electrical properties by TUNA of the formulated nanocomposites solidified by the same two-stage curing cycle were investigated. The electrical characterization by TUNA of the nanocomposites allowed to understand the correlation between the structure and the electrical properties of the nanometric domains and to evaluate the effectiveness of the dispersion of the conductive nanoparticles inside the epoxy matrix. Differential Scanning Calorimetry (DSC) was used to evaluate the degree of cure (DC) of the CNF1100 and CNF2500-based resins. All the samples analyzed showed a high DC of at least 90% perfectly meeting the requirements imposed by the aeronautical industry. The highest DC values that reached 100% even in isothermal conditions were obtained for the samples containing heat-treated carbon nanofibers. The high degree of cure of the nanofilled formulations was also confirmed by the cross-linking kinetics carried out by Fourier Transform Infrared Spectroscopy (FTIR). The attainment of good dispersion of carbon nanofibers within the matrix and strong interfacial adhesion at nanoscale which ensures uniform stress distribution together with the remarkable curing degree (around 100% for CNF2500/reinforced resins and higher than 90% for CNF1100/reinforced resins) are responsible for the relevant mechanical properties of the formulated nanocomposites. In particular, all the tested samples show a value in the storage modulus higher than 2000 MPa up to 110 °C and high values of the glass transition temperature ($\tan \delta$) centered between 260 and 280 °C, which are proper for structural applications.

Experimental

CNFs in the form of powders were produced at Applied Sciences Inc. and were from the Pyrograf III family. The pristine CNFs labeled CNF1100 (see morphological parameters of CNF1100 in Table S1 of the supporting information), were heat-treated at 2500 °C to provide the

best combination of mechanical and electrical properties [41], giving the sample CNF2500. For the preparation of the unfilled epoxy matrix, named EP, we mixed tetraglycidyl methylenedianiline (TGMDA, 80 mass%) with 1–4 butanediol diglycidyl ether (BDE, 20 mass%) and then solubilizing at 120 °C the hardener 4,4-diaminodiphenyl sulfone (DDS) in stoichiometric quantity. For the preparation of the nanofilled epoxy samples, CNF1100 and CNF2500 were added and ultrasonicated into the EP matrix at various mass% (0.05, 0.32, 0.64, 0.8, 1.0, 1.3, and up to 2.0 for CNF2500) giving the nanocomposites EP + X%nanofiller where X is the nanofiller (CNF1100 and CNF2500) mass percentage. All the mixtures were cured at 125 °C for 1 h and 200 °C for 3 h.

Characterizations

In this study, different characterization techniques such as Dynamic mechanical analysis (DMA), Fourier-transform infrared spectroscopy (FTIR), Differential Scanning Calorimetry (DSC), Thermogravimetric analysis (TGA), Field Emission Scanning Electron Microscopy (FESEM), electrical measurements of direct current (dc) conductivity, and TUNA analysis have been carried out. Detailed information on these characterization techniques is contained in the supporting information.

DSC has been employed to evaluate the degree of cure (DC) of the samples, assuming that exothermic heat developed during the curing process is proportional to the extent of the curing reactions. The DC has been obtained for samples cured in the dynamic regime, during the thermal scan directly in the DSC cell, and in the isothermal regime in an oven. Dynamic scans have been performed to analyze the degree of cure (DC) of the fresh (uncured) samples and of samples after the curing in the oven. The DC can be determined from the total heat of reaction (ΔH_T) of the curing reactions and the residual heat of reaction (ΔH_{Res}) of the partially cured resin according to Eq. 1 [42].

$$DC = \frac{\Delta H_T - \Delta H_{Res}}{\Delta H_T} \times 100 \quad (1)$$

The total heat of reaction (ΔH_T) has been determined by performing the DSC analysis on the liquid uncured resins, scanning about 7.0 mg of the sample by a heating run at 10 °C min⁻¹ from -50 to 300 °C, while the ΔH_{Res} was determined from the measurements performed on the oven hardened samples, by scanning the polymerized materials at 10 °C min⁻¹ from 0 to 300 °C.

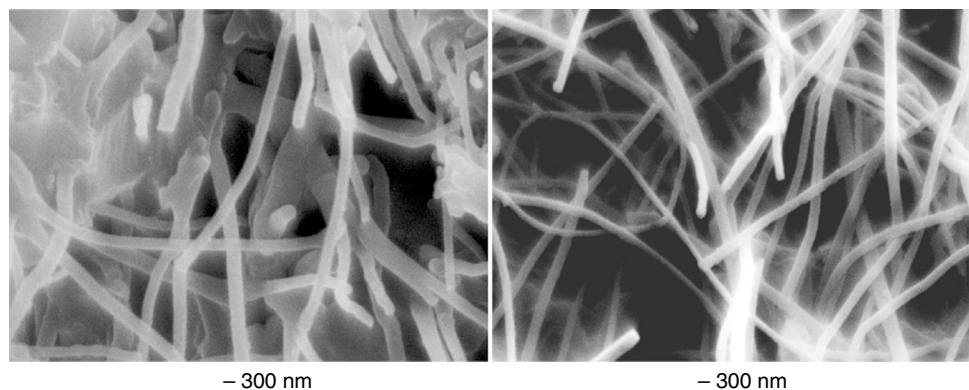
The analysis of the uncured samples was carried out by means of a dynamic heating program that contemplates three stages in the temperature range between -50 and 300 °C, namely: a) a first run from -50 up to 300 °C with a scan rate of 10 °C min⁻¹, b) a second run from 300 to -50 °C with a scan rate of 50 °C min⁻¹ and c) a third run from -50 up to 300 °C with a scan rate of 10 °C min⁻¹. The samples oven cured at 200 °C were analyzed by a single heating run from 0 up to 300 °C with a scan rate of 10 °C min⁻¹.

Results and discussion

FESEM investigation carried out on nanofilled samples highlights that CNF2500 (Fig. 1 on the right) seem to be characterized by a straighter structure and a smaller diameter than CNF1100 (Fig. 1 on the left). From the FESEM images, it is possible to see how the heat treatment at higher temperatures, by increasing the structural perfection of the nanofibers, has significantly influenced the change in their morphological characteristics and therefore also on the nanofiller-epoxy matrix interaction. In fact, the CNF2500 nanofibers appear less tightly bound to the matrix while instead most of the CNF1100 nanofibers show an intimate connection with the matrix due to the numerous functional groups present along the walls.

The heat treatment at 2500 °C also greatly influences the oxidative stability of the nanofibers, as can be seen from the thermogravimetric curves in air of the CNF1100 and

Fig. 1 FESEM images of EP + 1%CNF1100 (on the left) and EP + 1%CNF2500 nanocomposites (on the right)



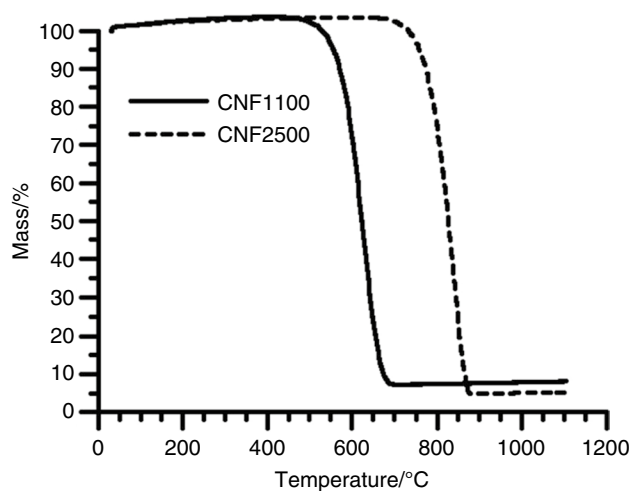


Fig. 2 TGA curves in air of CNF1100 and CNF2500

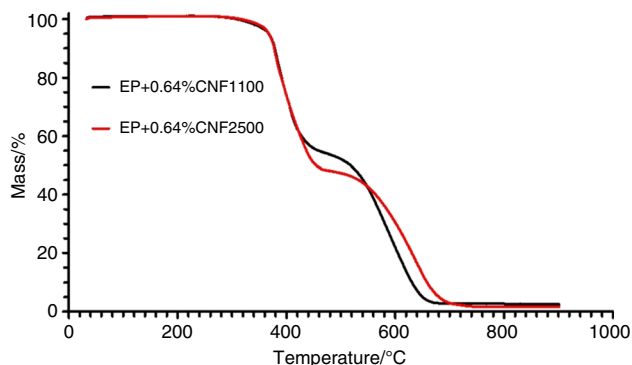


Fig. 3 TGA curves in air of solidified EP+0.64%CNF1100 and EP+0.64%CNF2500 nanocomposites

CNF2500 fillers (Fig. 2). We can observe that CNF2500s are more thermostable by about 200 °C than CNF1100s, since CNF2500s start to degrade at about 750 °C while the onset of thermal degradation of CNF1100 occurs at 550 °C. The more excellent thermal stability of the annealed CNF2500 is attributable to their greater structural perfection due to a reduced density of defects.

This different behavior is undoubtedly also due to the different chemical composition of the wall of the two types of carbon nanofibers. The reduced density of defect on the wall of CNF2500 is a direct consequence of an almost complete absence of functional groups that do not destroy the stacking of carbon layers. FTIR investigation supports this hypothesis [41].

Figure 3 shows the TGA curves in air of the nanofilled epoxy formulations EP + 0.64%CNF1100 and EP + 0.64%CNF2500.

The comparison between the two nanocomposites shows that the thermal treatment of the carbon nanofibers does not

influence the temperature at which the degradation begins. In fact, for both samples, the first oxidation stage occurs in the temperature range between 380 and 480 °C. Conversely, a strong influence of the different thermal treatments is instead revealed with respect to the electrical conductivity for the same nanofiller percentage of 0.64 mass% chosen to compare thermogravimetric properties with the electrical ones after the electrical percolation threshold (EPT), as can be seen from the dc conductivity values shown in the electrical characterization section shown later in the manuscript.

Figure 4a and b show the calorimetric curves of the EP resin and CNF1100-based nanocomposites solidified under dynamic conditions directly in the DSC cell and isothermal heating conditions in oven (see details in the experimental section), respectively.

Figure 5 shows the percentage of the degree of cure (DC) obtained for the CNF1100-based nanocomposites cured in the dynamic regime directly in the DSC cell and isothermal regime in oven.

For comparison, to emphasize the effect of heat treatment on CNFs, we have also reported the calorimetric curves of the EP resin and CNF2500-based nanocomposites solidified under dynamic conditions directly in the DSC cell (Fig. 6a) and isothermal heating conditions in oven (Fig. 6b).

Figure 7 shows the percentage of the degree of cure (DC) obtained for the CNF2500-based nanocomposites cured in the dynamic regime directly in the DSC cell and isothermal regime in oven.

The description of how the DC values were calculated is contained in the experimental section.

Figure 5 shows for the Epoxy/CNF1100 samples DC values higher than 90% also in the isothermal regime. Only for the CNF1100 mass percentage of 0.64, a slight decrease equal to 88% in the DC is observed. Figure 7 shows for the Epoxy/CNF2500 samples DC values higher than 97% also in the isothermal regime. For a mass percentage of nanofiller lower than 0.025, only a slight decrease in the DC value is observed. We can detect that the addition of the CNF2500 determines an increase in the curing process efficiency in the isothermal regime. Furthermore, all the samples filled with heat-treated CNF2500 show a DC value higher than that recorded for the unfilled EP resin, even reaching a value almost of 100%. This is most probably due to the heat treatment that acts effectively on the curing degree completely accomplishing the stringent conditions prevailing in the aviation industry.

The degree of cure (DC) of CNF2500 is higher because there are fewer chemical and attractive interactions with the host matrix, which are generally responsible for reducing the polyaddition reactions at the interface between the matrix and the nanofiller.

The effectiveness of the curing process was also demonstrated by the FTIR analysis performed for samples

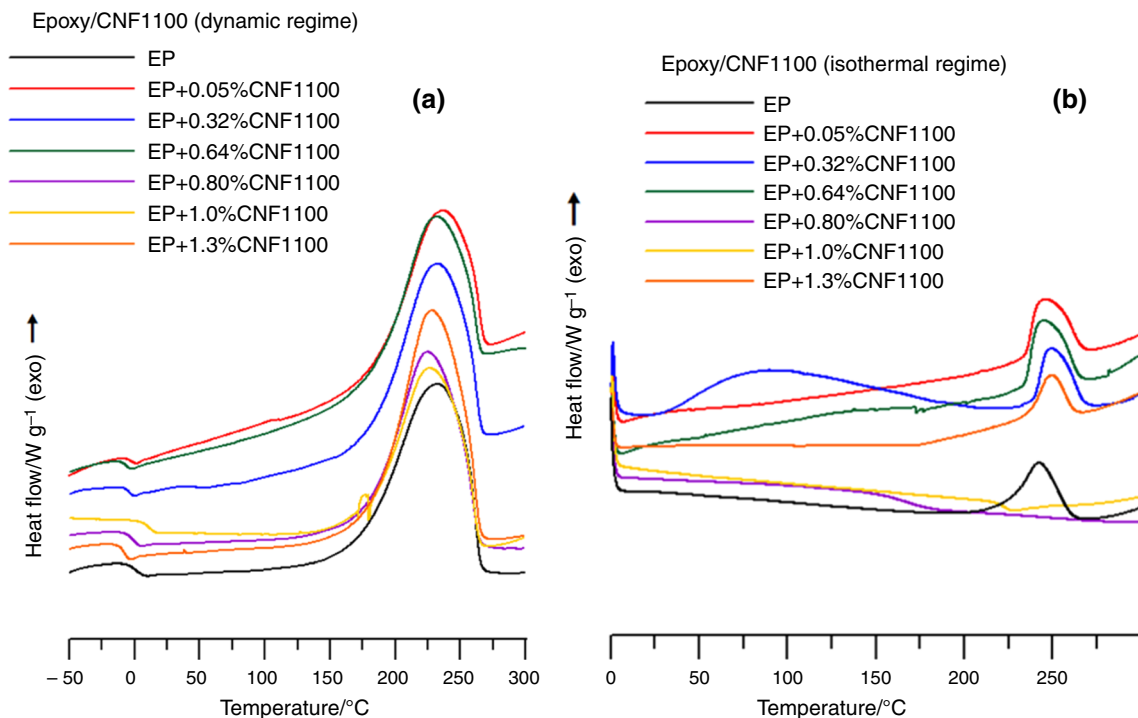


Fig. 4 **a** Calorimetric curves (dynamic regime) of the Epoxy/CNF1100 system; **b** Calorimetric curves (isothermal regime) of the Epoxy/CNF1100 system

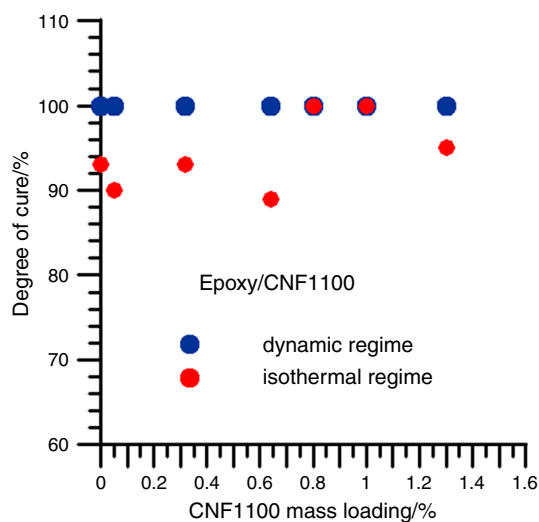


Fig. 5 Degree of cure/% of the Epoxy/CNF1100 system (dynamic and isothermal regimes)

EP + 1.0%CNF1100 (Fig. 8) and EP + 1.0%CNF2500 (Fig. 9) at different temperatures and times which are the same as foreseen by the curing cycle programmed for the samples examined in this study. The cross-linking kinetics allowed to demonstrate, through the change of the characteristic absorption peak of the epoxide group at 908 cm^{-1} , the complete cross-linking of the formulated materials. Observing

the evolution of the peak during the polymerization reaction, it can be seen that it is very marked at room temperature, less intense at $125\text{ }^{\circ}\text{C}$ after 1 h to then drop completely at $200\text{ }^{\circ}\text{C}$ after 3 h.

The storage modulus of the CNF1100- and CNF2500-based nanocomposites, compared with that of the unfilled epoxy resin EP, show a value that is higher than 2000 MPa up to $110\text{ }^{\circ}\text{C}$ for all the samples (Fig. 10a). For CNF2500-based samples, the reinforcing effect is detectable up to $60\text{ }^{\circ}\text{C}$. Instead, for the CNF1100-based samples, due to the intense intermolecular attractive interactions attributable to the hydrogen bonds that are established as a greater number of functional groups is present on the walls of the untreated CNF1100 nanofibers [41], a stronger reinforcing effect than the heat-treated CNF2500 in the temperature range (-90 to about $60\text{ }^{\circ}\text{C}$) is observable. The more marked strengthening effect shown by the composites based on CNF1100 in the temperature range (-90 to about $60\text{ }^{\circ}\text{C}$) can be attributed to the different morphological peculiarities of the CNFs.

This result implies that the nanocomposites exhibit more elastic behavior than the neat resin. It has been demonstrated that the presence of functional groups on the wall of nanofillers can determine covalent (es. etherification reactions and other ones) or non-covalent attractive interaction causing a reinforcing effect of nanofillers because the load is better transferred to the high-strength nanofiller [41]. This interpretation of the results perfectly agrees with the major

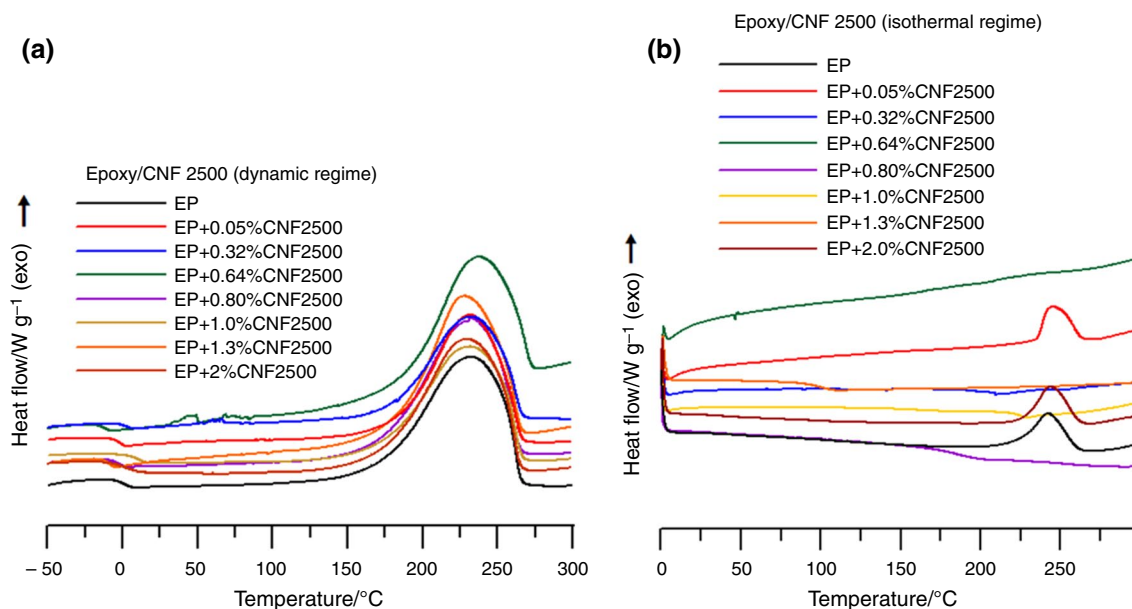


Fig. 6 **a** Calorimetric curves (dynamic regime) of the Epoxy/CNF2500 system; **b** Calorimetric curves (isothermal regime) of the Epoxy/CNF2500 system

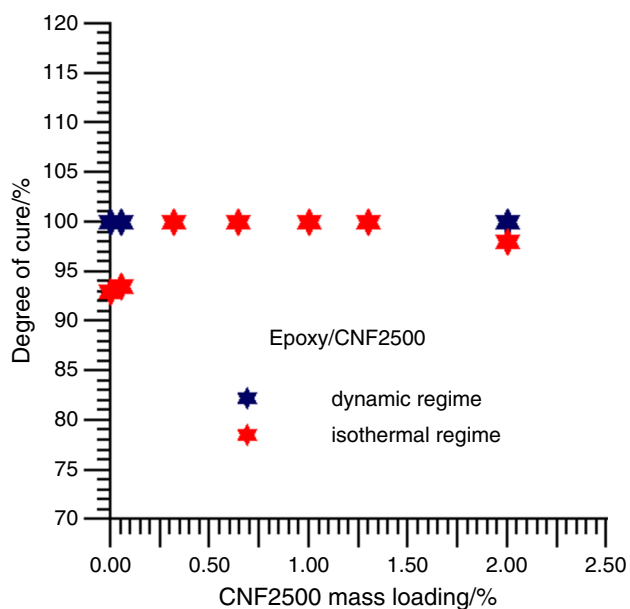


Fig. 7 Degree of cure/% of the Epoxy/CNF2500 system (dynamic and isothermal regimes)

increase determined by the CNF1100. On the other hand, the same effect was found with MWCNTs functionalized with -COOH groups [43].

Figure 10b shows $\tan \delta$ vs. T curves of the EP, EP+0.64%CNF1100, and EP+0.64%CNF2500 cured samples for which we can observe high values of the glass transition temperature ($\tan \delta$) centered between 260 and 280 °C.

The good mechanical properties exhibited by the carbon nanofiber-reinforced resins make them ideal candidates for a very vast range of structural applications.

The measured dc conductivity of the nanocomposites Epoxy/CNF1100 and Epoxy/CNF2500 as a function of the CNFs' mass percentage (Fig. 11) shows interesting results: samples loaded at $\nu = 0.05\%$ are effectively in a pre-percolation region. The dc conductivity of the nanocomposites Epoxy/CNF1100 and Epoxy/CNF2500 is around $6.5 \times 10^{-13} \text{ S m}^{-1}$ and $5.1 \times 10^{-13} \text{ S m}^{-1}$ respectively; whereas, the unfilled matrix exhibits a conductivity $\nu = 6.0 \times 10^{-14} \text{ S m}^{-1}$. As for the composite filled with CNTs [41], the samples at $\nu = 1.0\%$ of CNFs are characterized by high dc conductivity with respect to the unfilled material, i.e., $\nu = 1.36 \times 10^{-3} \text{ S m}^{-1}$ (sample filled with CNF1100) and $\nu = 0.107 \text{ S m}^{-1}$ (sample filled with CNF2500), respectively. The increase in dc conductivity is approximately three orders of magnitude after the heat treatment undergone by the carbon nanofibers. The dc value for $\nu = 0.32\%$ evidences an important effect of the different treatments of the two fillers: the composite filled with CNF1100 treated at a lower temperature is still in the "insulator" region, whereas for the higher temperature, it is already in the "conductor" region. In fact, the dc conductivity is less than $10^{-12} \text{ S m}^{-1}$ for the CNF1100 composite whereas a dc conductivity almost similar to the value obtained for $\nu = 1.0\%$ sample is measured for the CNF2500 composite, i.e., $2.5 \times 10^{-2} \text{ S m}^{-1}$. This corresponds to assure that the concentration $\nu = 0.32\%$ is a left extreme value for the region of percolation threshold

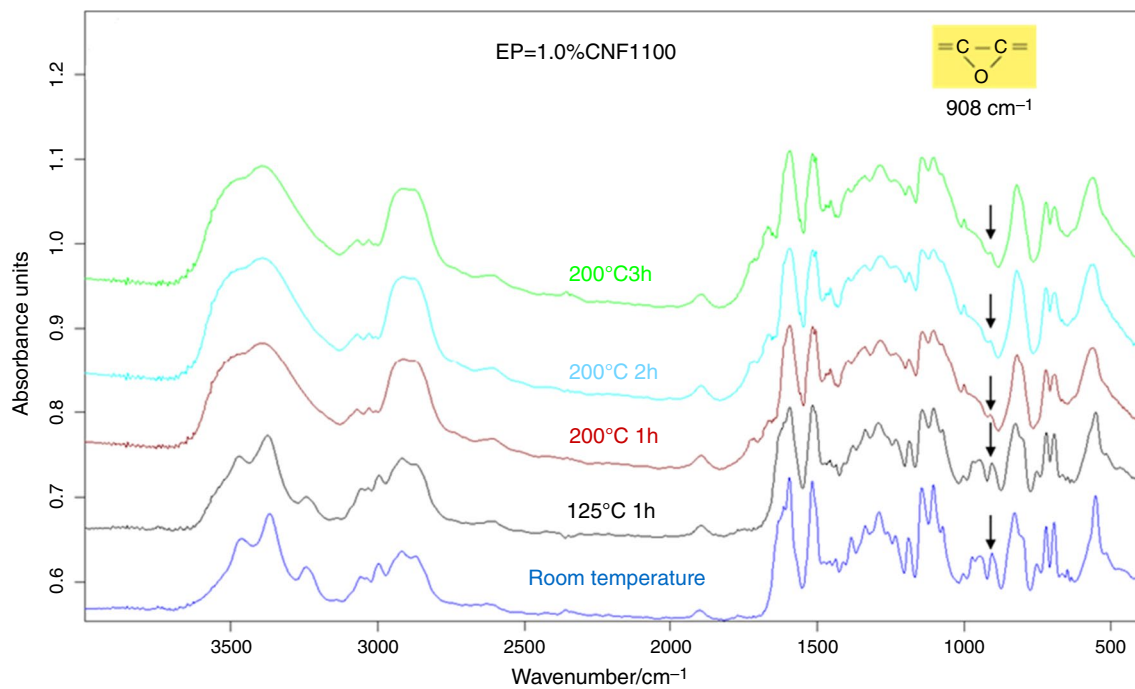


Fig. 8 FTIR spectra of EP + 1%CNF1100 formulation at different temperatures and times of curing reactions

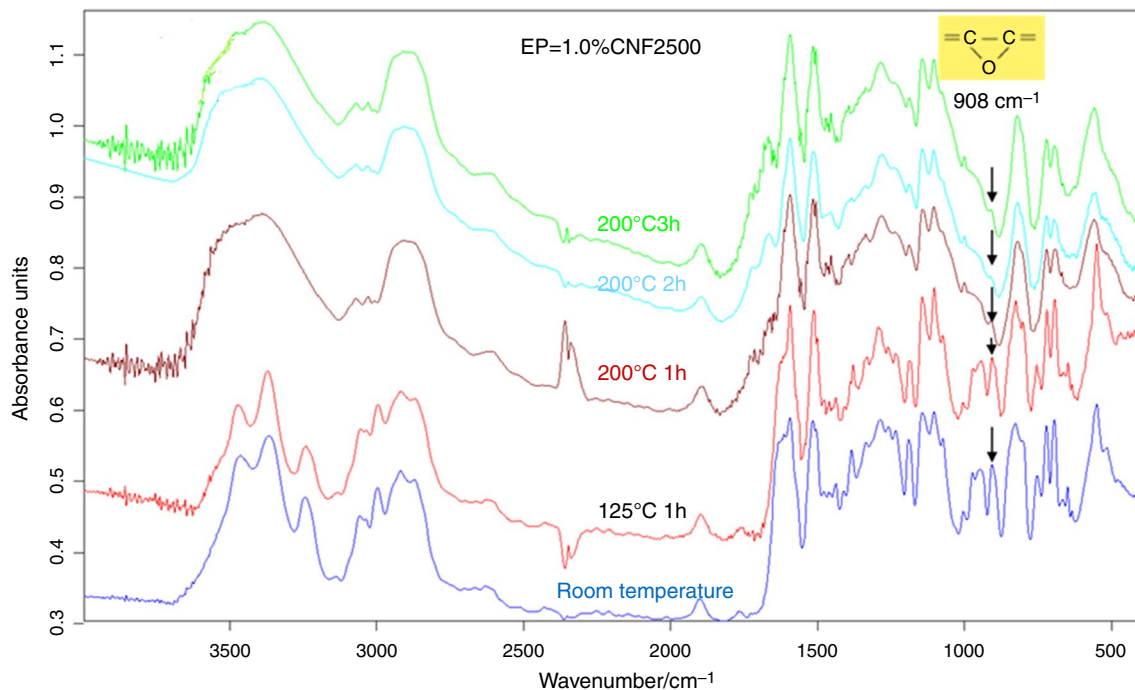


Fig. 9 FTIR spectra of EP + 1%CNF2500 formulation at different temperatures and time of curing reactions

of the CNF1100, i.e., $\nu_{c-CNF1100} \in [0.32, 1]\%$, whereas it represents a right extreme value for the CNF2500, i.e., $\nu_{c-CNF2500} \in [0.05, 0.32]\%$. As a result of the heat treatment, high values in electrical conductivity are obtained

for a smaller amount of nanofiller. Furthermore, a smaller amount is needed to reach the EPT relative to the electrical percolation threshold.

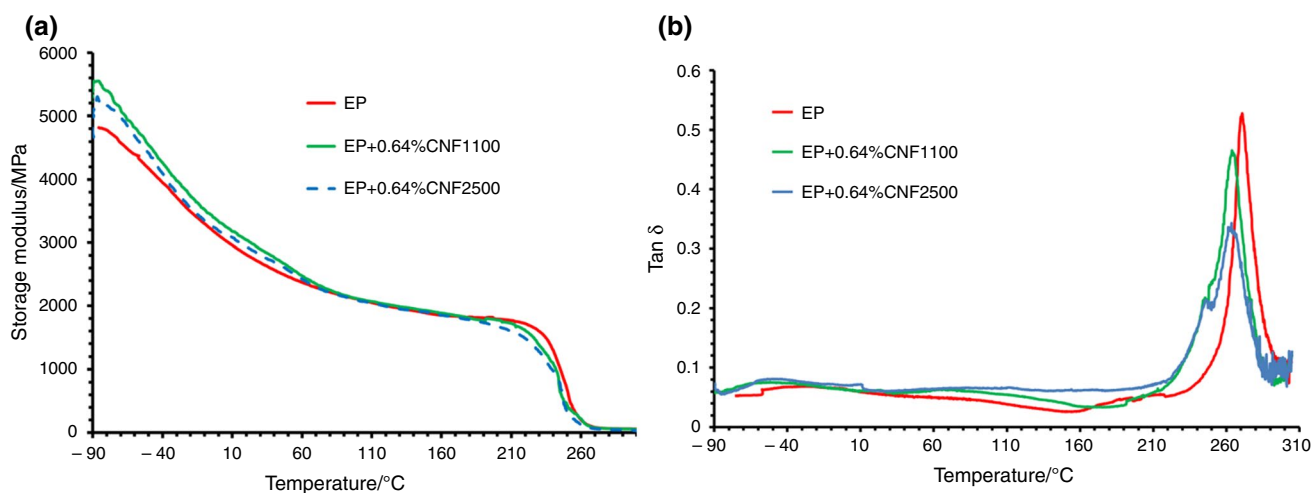


Fig. 10 **a** Storage modulus vs. T curves of the EP, EP+0.64%CNF1100 and EP+0.64%CNF2500 cured samples; **b** Tan δ vs. T curves of the EP, EP+0.64%CNF1100, and EP+0.64%CNF2500 cured samples

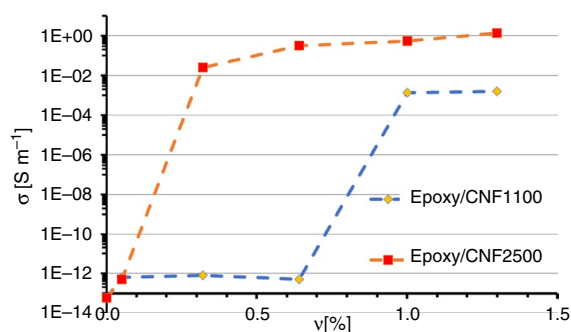


Fig. 11 Dc conductivity of the Epoxy/CNF1100 and Epoxy/CNF2500 nanocomposites versus CNF mass percentage

In order to correlate the local topography with the electrical properties of the nanocomposites filled with pristine and heat-treated CNFs, and to evaluate the effectiveness of nanofiller dispersion within the polymeric matrix we performed a

morphological characterization by TUNA. In this study, we report the TUNA images of the samples EP + 1.0%CNF1100 and EP + 1.0%CNF2500 where the chosen nanofiller amount of 1.0 mass% is above the EPT. For these samples, the conductivity values of $1.36 \times 10^{-3}\ S\ m^{-1}$ and $0.107\ S\ m^{-1}$ were measured, respectively. In this regard, Figs. 12 and 13 show the bidimensional (2D) and tridimensional (3D) profiles of the TUNA Current images of EP + 1.0%CNF1100 and EP + 1.0%CNF2500, respectively.

For both analyzed nanocomposites, the percentage of 1.0 mass% of nanofiller that is above the electrical percolation threshold was chosen. We can clearly observe a rather homogeneous distribution of the nanofiller within the matrix for the two samples analyzed. From Fig. 12, it is evident that the CNF1100 nanofibers are more intensely anchored to the epoxy matrix with which strong intermolecular interactions are established due to hydrogen bonds. The presence of the nanofibers emerging from the areas of interconnection with the matrix is easily discriminated by

Fig. 12 TUNA Current image of EP + 1.0%CNF1100: **a** bidimensional (2D) profile; **b** tridimensional (3D) profile

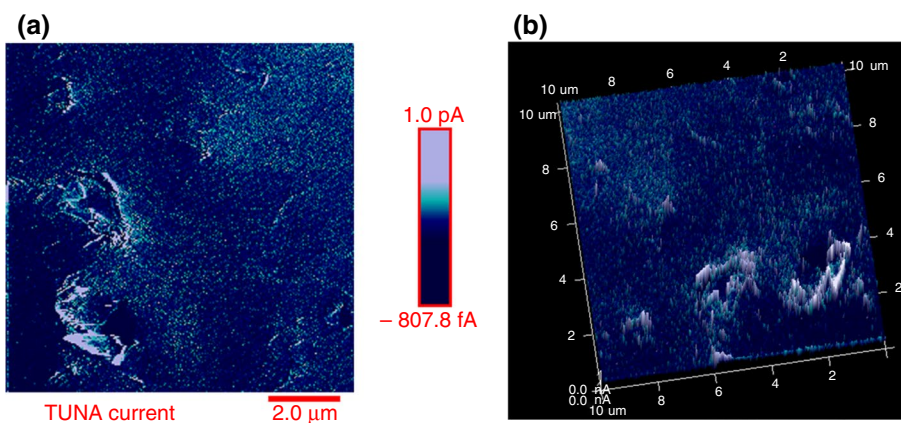
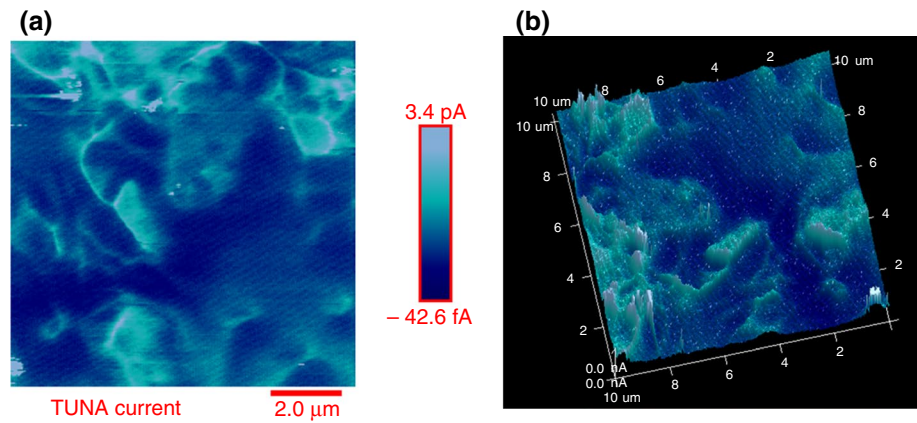


Fig. 13 TUNA Current image of EP + 1.0%CNF2500: **a** bidimensional (2D) profile; **b** tridimensional (3D) profile



appearing on the surface with a lighter color with which a higher value of the electric current is associated. In fact, the scale bar extends over a range of colors that go from darkest to lightest in correspondence with areas of lower and higher local electrical conductivity. For sample EP + 1.0%CNF1100 for which a dc conductivity equal to $1.36 \times 10^{-3} \text{ S m}^{-1}$ was measured, the electric current values range from -807.8 fA to 1 pA (Fig. 12), while for sample EP + 1.0%CNF2500 for which a dc conductivity equal to 0.107 S m^{-1} was measured, the values of electric current range from -42.6 fA to 3.4 pA (Fig. 13). For sample EP + 1.0%CNF2500, a network of nanofibers appearing with a light blue color is observed which extends branching along the entire investigated surface giving rise to a highly crosslinked three-dimensional structure (Fig. 13). In this way, an excellent transfer of the electrical properties to the insulating matrix is ensured thanks to the current flow due to the tunnel effect charged by the conductive nanofibers.

The TUNA Current image also allows for obtaining information on the dispersion of carbon nanofibers in the resin. In this regard, Figs. 14 and 15 show the profile of the current variations (see green, red, and blue colors on the right picture) correlated with the TUNA current images (see the three white lines on the left picture) of EP + 1.0%CNF1100 and EP + 1.0%CNF2500, respectively. It can easily be seen how the carbon nanofibers are well distributed within the matrix by observing how the frequency of the current variations attributable to the filler/matrix interchanges along the 3 white lines is rather constant for both nanocomposites analyzed. In particular, in correspondence with some nanodomains characterized by a higher electric charge density, the current variations are more intense for the sample EP + 1.0%CNF2500 (Fig. 15) which shows higher conductivity values as a consequence of the presence of the CNF2500 endowed with a greater intrinsic conductivity.

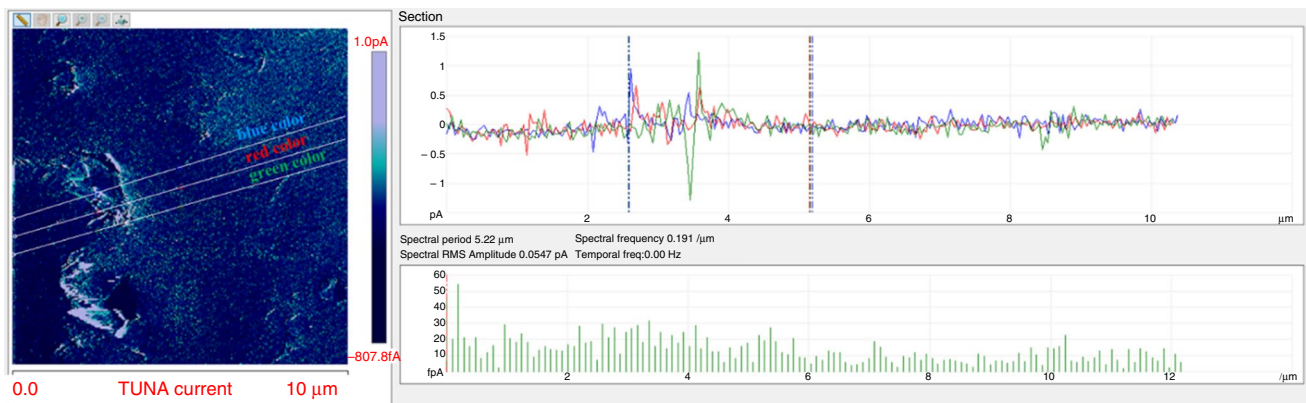


Fig. 14 Profile of the current variations of EP + 1.0%CNF1100

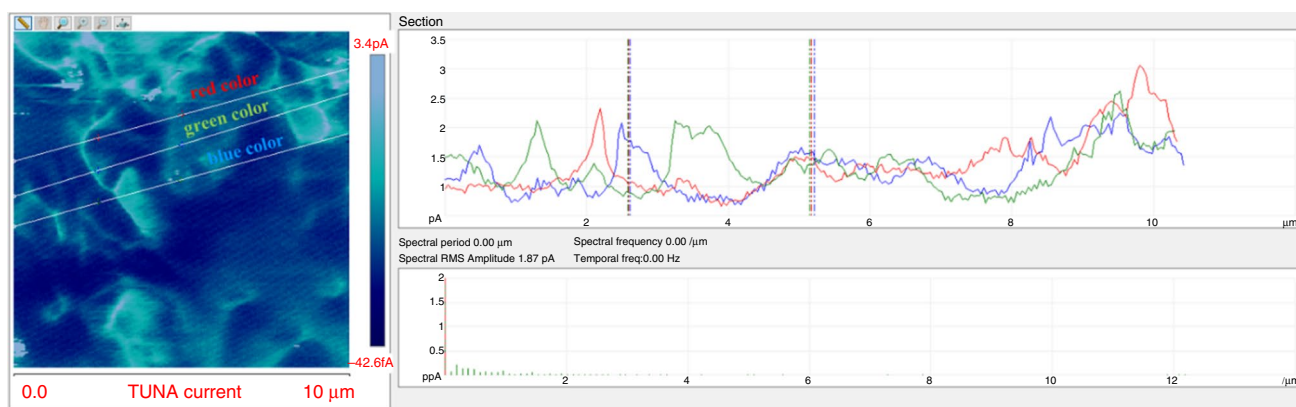


Fig. 15 Profile of the current variations of EP + 1.0%CNF2500

Conclusions

A comparative study between various characterizations has demonstrated that the thermal, electrical, and mechanical properties of the nanocomposites based on CNFs are strongly influenced by the heat treatment of carbon nanofibers. Heat treatment at 2500 °C removes the defects on the walls of CNFs, increasing their structural perfection with a consequent increase in the nanocomposites' electrical conductivity at low filler concentration values. A less marked increase in the storage modulus is observed compared with the nanocomposites filled with nanofibers obtained at 1100 °C. Both the composites' typologies manifest higher storage modulus values than the unfilled resin.

The dc conductivity value for $\nu=0.32\%$ is less than 10^{-12} S m⁻¹ for the CNF1100 composite, whereas a dc conductivity similar to the value obtained for $\nu=1.0\%$ sample is measured for the CNF2500 based composite, i.e., 2.5×10^{-2} S m⁻¹. The more marked strengthening effect shown by the composites based on CNF1100 in the temperature range (−90 to about 60 °C) can be attributed to the different morphological peculiarities of the CNFs. Furthermore, the heat treatment at 2500 °C, while increasing the nanofiller's oxidative stability, leaves the nanocomposites' stability practically unchanged. The highest DC, which reaches 100% even in isothermal curing conditions, was recorded for CNF2500-based nanocomposites, thus allowing a highly crosslinked structure. TUNA analysis provides for identifying a very good nanoscopic distribution of the conductive phase within the host matrix, thus allowing a compelling correlation of the composites' multifunctional properties.

Supplementary Information The online version contains supplementary material available at <https://doi.org/10.1007/s10973-023-12521-6>.

Authors' Contribution The authors have no conflicts of interest to declare that are relevant to the content of this article.

Funding Open access funding provided by Università degli Studi di Salerno within the CRUI-CARE Agreement. **Open Access** This article is licensed under a Creative Commons Attribution 4.0 International License, which permits use, sharing, adaptation, distribution and reproduction in any medium or format, as long as you give appropriate credit to the original author(s) and the source, provide a link to the Creative Commons licence, and indicate if changes were made. The images or other third party material in this article are included in the article's Creative Commons licence, unless indicated otherwise in a credit line to the material. If material is not included in the article's Creative Commons licence and your intended use is not permitted by statutory regulation or exceeds the permitted use, you will need to obtain permission directly from the copyright holder. To view a copy of this licence, visit <http://creativecommons.org/licenses/by/4.0/>.

References

- Zhang F, Zong L, Weng Z, Bao F, Li N, Wang J, Jian X. Highly enhanced performance of epoxy composites via novel phthalazinone-bearing hybrid system as matrix. *Compos Part A Appl Sci Manuf.* 2020;131:105772. <https://doi.org/10.1016/j.compositesa.2020.105772>.
- Sinh LH, Trung NN, Son BT, Shin S, Thanh DT, Bae JY. Curing behavior, thermal, and mechanical properties of epoxy resins cured with a novel liquid crystalline dicarboxylic acid curing agent. *Polym Eng Sci.* 2014;54(3):695–703. <https://doi.org/10.1002/pen.23585>.
- Jena RK, Yue CY, Sk MM, Ghosh K. A novel high performance bismaleimide/diallyl bisphenol A (BMI/DBA)–epoxy interpenetrating network resin for rigid riser application. *Rsc Adv.* 2015;5(97):79888–97. <https://doi.org/10.1039/c5ra14474d>.
- Raimondo M, Donati G, Milano G, Guadagno L. Hybrid composites based on carbon nanotubes and graphene nanosheets outperforming their single-nanofiller counterparts. *FlatChem.* 2022;36:100431. <https://doi.org/10.1016/j.flatc.2022.100431>.
- Guadagno L, Pantelakis S, Strohmayer A, Raimondo M. High-performance properties of an aerospace epoxy resin loaded with carbon nanofibers and glycidyl polyhedral oligomeric silsesquioxane. *Aerospace.* 2022;9(4):222. <https://doi.org/10.3390/aerospace9040222>.
- Loos MR, Ferreira Coelho LA, Pezzin SH, Amico SC. Effect of carbon nanotubes addition on the mechanical and thermal

- properties of epoxy matrices. *Mater Res.* 2008;11(3):347–52. <https://doi.org/10.1590/S1516-14392008000300019>.
7. Blanco I, Cicala G, Faro CL, Recca A. Development of a toughened DGEBS/DDS system toward improved thermal and mechanical properties by the addition of a tetrafunctional epoxy resin and a novel thermoplastic. *J Appl Polym Sci.* 2003;89(1):268–73. <https://doi.org/10.1002/app.12179>.
 8. Blanco I, Cicala G, Faro CL, Motta O, Recca G. Thermomechanical and morphological properties of epoxy resins modified with functionalized hyperbranched polyester. *Polym Eng Sci.* 2006;46(11):1502–11. <https://doi.org/10.1002/pen.20604>.
 9. Blanco I, Cicala G, Motta O, Recca A. Influence of a selected hardener on the phase separation in epoxy/thermoplastic polymer blends. *J Appl Polym Sci.* 2004;94(1):361–71. <https://doi.org/10.1002/app.20927>.
 10. Zhou YX, Pervin F, Lewis L, Jeelani S. Experimental study on the thermal properties of multi-walled carbon nanotube reinforced epoxy. *Mater Sci Eng A.* 2007;452:657–64. <https://doi.org/10.1016/j.msea.2006.11.066>.
 11. Sheinbaum M, Sheinbaum L, Weizman O, Dodiuk H, Kenig S. Toughening and enhancing mechanical and thermal properties of adhesives and glass-fiber reinforced epoxy composites by brominated epoxy. *Compos B Eng.* 2019;165:604–12. <https://doi.org/10.1016/j.compositesb.2019.02.020>.
 12. Santos P, Maceiras A, Valvez S, Reis PNB. Mechanical characterization of different epoxy resins enhanced with carbon nanofibers. *Frattura ed Integrità Strutturale.* 2021;55:198–212. <https://doi.org/10.3221/IGF-ESIS.55.15>.
 13. Tian Y, Wang Q, Shen L, Cui Z, Kou L, Cheng J, Zhang J. A renewable resveratrol-based epoxy resin with high T_g, excellent mechanical properties and low flammability. *Chem Eng J.* 2020;383:123124. <https://doi.org/10.1016/j.cej.2019.123124>.
 14. Zhang J, Yao T, Shahsavarian T, Li C, Lei Z, Zhang Z, Jia R, Diahm S. Improvement in anti-static property and thermal conductivity of epoxy resin by doping graphene. *IEEE Trans Dielectr Electr Insul.* 2020;27:542–8. <https://doi.org/10.1109/TDEI.2020.008620>.
 15. Liu YD, Wang ZG. Thermal and dielectric properties of nanocomposites prepared from reactive graphene oxide and silicon-containing cycloaliphatic diepoxide. *Polym Compos.* 2020;41:871–8. <https://doi.org/10.1002/pc.25417>.
 16. Raimondo M, Naddeo C, Catauro M, Guadagno L. Thermo-mechanical properties and electrical mapping of nanoscale domains of carbon-based structural resins. *J Therm Anal Calorim.* 2022;147(9):5473–81. <https://doi.org/10.1007/s10973-021-11176-5>.
 17. Nobile MR, Raimondo M, Naddeo C, Guadagno L. Rheological and morphological properties of non-covalently functionalized graphene-based structural epoxy resins with intrinsic electrical conductivity and thermal stability. *Nanomaterials.* 2020;10:1310. <https://doi.org/10.3390/nano10071310>.
 18. Pistone A, Scolaro C, Visco A. Mechanical properties of protective coatings against marine fouling: a review. *Polymers.* 2021;13:173. <https://doi.org/10.3390/polym13020173>.
 19. Karlsson AM, Adeoye MO. Composites, multifunctional. In: Meyers R, editor. *Encyclopedia of complexity and systems science.* New York: Springer; 2009.
 20. Jagath Narayana K, Burela RG. A review of recent research on multifunctional composite materials and structures with their applications. *Mater Today Proc.* 2018;5(2):5580–90. <https://doi.org/10.1016/j.matpr.2017.12.149>.
 21. Utekar S, Suriya VK, More N, Rao A. Comprehensive study of recycling of thermosetting polymer composites-Driving force, challenges and methods. *Compos Part B Eng.* 2021;207:108596. <https://doi.org/10.1016/j.compositesb.2020.108596>.
 22. Post W, Susa A, Blaauw R, Molenveld K, Knoop RJ. A review on the potential and limitations of recyclable thermosets for structural applications. *Polym Rev.* 2020;60(2):359–88. <https://doi.org/10.1080/15583724.2019.1673406>.
 23. Klingler WW, Bifulco A, Polisi C, Huang Z, Gaan S. Recyclable inherently flame-retardant thermosets: chemistry, properties and applications. *Compos Part B Eng.* 2023;258:110667. <https://doi.org/10.1016/j.compositesb.2023.110667>.
 24. Morici E, Dintcheva NT. Recycling of thermoset materials and thermoset-based composites: challenge and opportunity. *Polymers.* 2022;14:4153. <https://doi.org/10.3390/polym14194153>.
 25. Onyancha R, Aigbe U, Ukhurebor K, Muchiri P. Facile synthesis and applications of carbon nanotubes in heavy-metal remediation and biomedical fields: a comprehensive review. *J Mol Struct.* 2021;1238:130462. <https://doi.org/10.1016/j.molstruc.2021.130462>.
 26. Manawi Y, Samara A, Al-Ansari T, Atieh M. A review of carbon nanomaterials' synthesis via the chemical vapor deposition (CVD) method. *Materials.* 2018;11(5):822. <https://doi.org/10.3390/ma11050822>.
 27. Onyancha RB, Ukhurebor KE, Aigbe UO, Osibote OA, Kusuma HS, Darmokoesoemo H. A methodical review on carbon-based nanomaterials in energy-related applications. *Adsorpt Sci Technol.* 2022;2022:4438286. <https://doi.org/10.1155/2022/4438286>.
 28. Rahman MM, Islam M, Roy R, Younis H, AlNahyan M, Younes H. Carbon nanomaterial-based lubricants: review of recent developments. *Lubricants.* 2022;10:281. <https://doi.org/10.3390/lubricants10110281>.
 29. Nunna S, Ravindran AR, Mrosczcok J, Creighton C, Varley RJ. A review of the structural factors which control compression in carbon fibres and their composites. *Compos Struct.* 2023;303:116293. <https://doi.org/10.1016/j.compstruct.2022.116293>.
 30. Kolahdouz M, Xu B, Nasiri AF, Fathollahzadeh M, Manian M, Aghababa H, Wu Y, Radamson HH. Carbon-related materials: graphene and carbon nanotubes in semiconductor applications and design. *Micromachines (Basel).* 2022;13(8):1257. <https://doi.org/10.3390/mi13081257>.
 31. Szczurek A, Barcikowski M, Leluk K, Babiarczuk B, Kaleta J, Krzak J. Improvement of interaction in a composite structure by using a sol-gel functional coating on carbon fibers. *Materials.* 2017;10(9):990. <https://doi.org/10.3390/ma10090990>.
 32. Bokov D, Turki Jalil A, Chupradit S, Suksatan W, Javed Ansari M, Shewael IH, Valiev GH, Kianfar E. Nanomaterial by sol-gel method: synthesis and application. *Adv Mater Sci Eng.* 2021;2021:5102014. <https://doi.org/10.1155/2021/5102014>.
 33. Vertuccio L, Guadagno L, D'Angelo A, Viola V, Raimondo M, Catauro M. Sol-gel synthesis of caffeic acid entrapped in silica/polyethylene glycol based organic-inorganic hybrids: drug delivery and biological properties. *Appl Sci.* 2023;13(4):2164. <https://doi.org/10.3390/app13042164>.
 34. Rahman IA, Padavettan V. Synthesis of silica nanoparticles by sol-gel: size-dependent properties, surface modification, and applications in silica-polymer nanocomposites—a review. *J Nanomater.* 2012;2012:132424. <https://doi.org/10.1155/2012/132424>.
 35. Coleman JN, Khan U, Gunko YK. Mechanical reinforcement of polymers using carbon nanotubes. *Adv Mater.* 2006;18(6):689–706. <https://doi.org/10.1002/adma.200501851>.
 36. Xie XL, Mai YW, Zhou XP. Dispersion and alignment of carbon nanotubes in polymer matrix: a review. *Mater Sci Eng R.* 2005;49(4):89–112. <https://doi.org/10.1016/j.mser.2005.04.002>.
 37. Guadagno L, Vertuccio L, Sorrentino A, Raimondo M, Naddeo C, Vittoria V, et al. Mechanical and barrier properties of epoxy resin filled with multi-walled carbon nanotubes. *Carbon.*

- 2009;47(10):2419–30. <https://doi.org/10.1016/j.carbon.2009.04.035>.
38. Guadagno L, De Vivo B, Di Bartolomeo A, Lamberti P, Sorrentino A, Tucci V, et al. Effect of functionalization on the thermo-mechanical and electrical behavior of multi-wall carbon nanotube/epoxy composites. *Carbon*. 2011;49(6):1919–30. <https://doi.org/10.1016/j.carbon.2011.01.017>.
39. Sandler JKW, Kirk JE, Kinloch IA, Shaffer MSP, Windle AH. Ultra-low electrical percolation threshold in carbon-nanotube-epoxy composites. *Polymer*. 2003;44(19):5893–9. [https://doi.org/10.1016/S0032-3861\(03\)00539-1](https://doi.org/10.1016/S0032-3861(03)00539-1).
40. Khare R, Bose S. Carbon nanotube based composites-a review. *J Min Mater Charact Eng*. 2005;4(1):31–46. <https://doi.org/10.4236/jmmce.2005.41004>.
41. Guadagno L, Raimondo M, Vittoria V, Vertuccio L, Lafdi K, De Vivo B, Lamberti P, Spinelli G, Tucci V. The role of carbon nanofiber defects on the electrical and mechanical properties of CNF-based resins. *Nanotechnology*. 2013;24:305704. <https://doi.org/10.1088/0957-4484/24/30/305704>.
42. Raimondo M, Guadagno L, Vertuccio L, Naddeo C, Barra G, Spinelli G, Lamberti P, Tucci V, Lafdi K. Electrical conductivity of carbon nanofiber reinforced resins: potentiality of tunneling atomic force microscopy (TUNA) technique. *Compos Part B Eng*. 2018;143:148–60. <https://doi.org/10.1016/j.compositesb.2018.02.005>.
43. Guadagno L, De Vivo B, Di Bartolomeo A, Lamberti P, Sorrentino A, Tucci V, Vertuccio L, Vittoria V. Effect of functionalization on the thermo-mechanical and electrical behavior of multi-wall carbon nanotube/epoxy composites. *Carbon*. 2011;49:1919–30. <https://doi.org/10.1016/j.carbon.2011.01.017>.

Publisher's Note Springer Nature remains neutral with regard to jurisdictional claims in published maps and institutional affiliations.